ASPECTS CONCERNING THE COMMUTATION OF 8/6 SWITCHED RELUCTANCE MOTORS

V. Trifa, Ramona Gălătuş, A. Szekely, Cs. Szasz

Technical University of Cluj-Napoca, Romania

Abstract - Principles of commutation logic for 4-phase 8/6 switched reluctance motors (SRM) are analyzed starting from a given angular transducer configuration. This configuration ensures five modes of phase control: normal, boost, long-dwell, two-phase-on and brake, with 4-quadrant operation of SRM. The control modes are simulated using Simulink environment on a model consisting in SRM with a 4-sensor optical transducer and a unipolar PWM inverter. A set of curves is presented and a comparison with experimental results is given.

Keywords : switched reluctance motor, optical transducer, logic control, numerical simulation, 4-quadrant operation, mechanical characteristics.

1. INTRODUCTION

Commutation process of SRM is one of the most important problem that occurs when experimenting its behaviour. This process ensures proper operation and allows developing high speed with acceptable torque ripples and noise. Recent studies are usually devoted to two aspects: 1. To find the optimal switching angle of phase control and 2. To process the transducer signals for obtaining various control modes in 4-quadrant operation. The paper refers to both aspects, insisting on the second problem.
Geometrical features of SRM are depicted in figure 1.

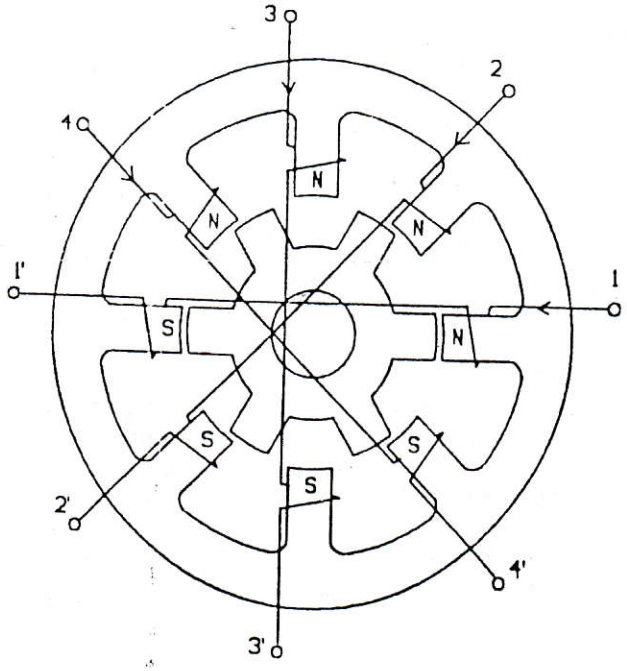

Figure 1. SRM stator-rotor configuration

The rotor is represented in the aligned position of phase 11' that is for maximal inductivity of this phase. The 8 stator poles are wound so that each phase consists in two diametrically opposite windings. This 4-phase arrangement determines mutual inductivities practically null and in this way an important simplification of SRM model is attained. Other modes of connecting the stator windings are possible [1].

2. TRANSDUCER STRUCTURE

A 4-quadrant operation of SRM is achieved when a 4-sensor transducer is chosen. In the case of 4-phase 8/6 SRM the 4 opto-electronic sensor are placed on the stator, as shown in figure 2.

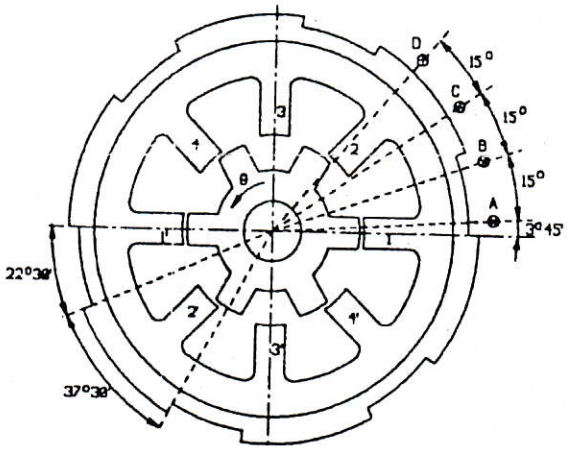

Figure 2. 4-sensor placement in the angular transducer

The 4 -sensor axes A-B-C-D are respectively shifted with 15° starting with a commutation angle calculated with [2]:

$$\theta_{sh} = \frac{180^0}{2Sz_r} = 3.75^0 \qquad (1)$$

where S is the number of sensors (S=4) and z_r is the number of rotor poles (z_r=6). A slotted disk mounted on rotor shaft contains 6 teeth of $30^0+2\theta_{sh}=37.5^0$ and 6 slots of $30^0-2\theta_{sh}=22.5^0$. This configuration enables a symmetrical operation in forward/reverse directions.

3. COMMUTATION LOGIC

By logical processing of transducer signals the control pulses for the inverter that supplies the SRM phases are deduced. With a commutation angle of 3.75^0 as shown above, there are more control modes, depending on the switch-on and switch-off angles with respect to unaligned rotor positions (minimal phase inductivity). Figure 3 shows phase control pulses in 1-phase-on, long-dwell and 2-phase-on driving.

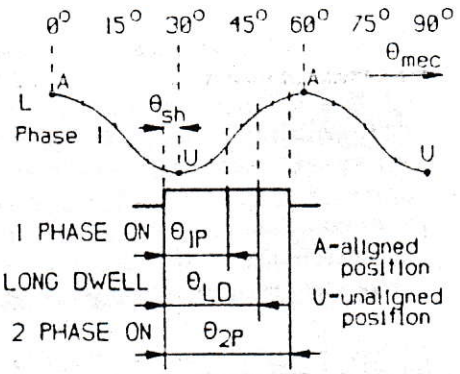

Figure 3. Commutation control pulses

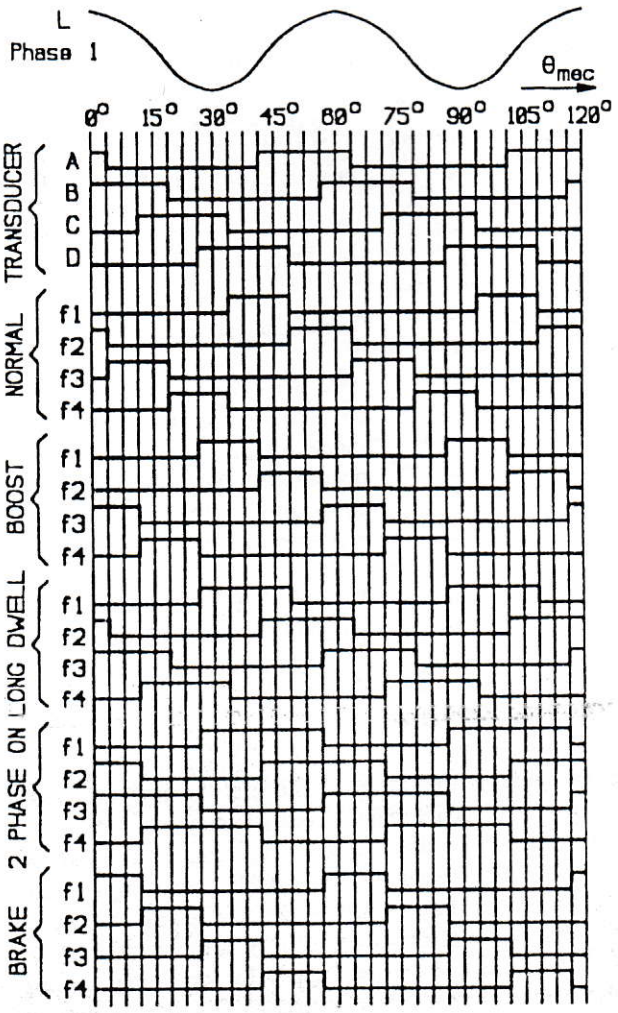

Figure 4. Multimode control signals for the inverter

The variation of phase 1 inductivity is taken as reference and a start angle of 3.75^0 before unaligned position is considered. 1-phase-on driving corresponds to single phase sequential supplying (θ_{1P}), long-dwell driving is for partial overlapping supplying (θ_{LD}) and 2-phase-on is for two phase sequential supplying (θ_{2P}). In all three modes the phase current starts building up before the inductivity begins to increase and ends on the positive slope of inductivity. Multimode control signals are deduced from transducer signals A-B-C-D, as illustrated in figure 4.

The inverter control signals f1÷f4 are represented taking as reference the variation of phase 1 inductivity. The five modes: normal, boost, long-dwell, 2-phase-on, brake are portrayed in forward rotor direction (trigonometric sense). These modes are discussed below:

a) normal mode: the switch-on angle occurs at 3.75^0 after the unaligned position of phase 1 (30^0) and the switch-off angle occurs 15^0 later, at 48.75^0;

b) boost mode: the switch-on angle occurs at 3.75^0 before the unaligned rotor position, at 26.25^0 and the switch-off angle occurs at 41.25^0;

c) long-dwell mode: the switch-on angle is the same as in boost mode, at 26.25^0, but the switch-off angle is at 48.25^0. In this case partial overlapping of $2x3.75^0$ of phase supply is obtained;

d) 2-phase-on mode: the switch-on angle is the same as above, at 26.25^0, while the switch-off angle occurs 30^0 later, at 56.25^0. Classical 2-phase-on driving is obtained with a commutation angle of 3.75^0;

e) Brake mode: the switch-on angle takes place at 3.75^0 before the aligned rotor position (60^0) and the switch-off angle occurs 15^0 later, at 71.25^0, that is on the negative slope of inductivity.

Normal, boost and brake modes correspond to one-phase-on driving, long-dwell mode to partial current overlapping of $2\theta_{sh}=7.5^0$ and 2-phase-on mode to a current overlapping of $4\theta_{sh}=15^0$. The five control modes are obtained by logical combinations of transducer signals A-B-C-D, as given in table 1.

Combinatorial logic for providing inverter control signals can be implemented by PROM or PLA memories, or by a

Table 1

phase	normal	boost	long-dwell	2-phase-on	brake
f1	$\bar{B}\bar{C}D$	$\bar{A}\bar{B}D$	D	D+$A\bar{B}$	$B\bar{C}\bar{D}$
f2	$A\bar{C}\bar{D}$	$A\bar{B}\bar{C}$	A	A+$\bar{C}\bar{D}$	$\bar{A}C\bar{D}$
f3	$\bar{A}B\bar{D}$	$B\bar{C}\bar{D}$	B	B+$C\bar{D}$	$\bar{A}\bar{B}D$
f4	$\bar{A}\bar{B}C$	$\bar{A}C\bar{D}$	C	C+$\bar{A}\bar{B}$	$A\bar{B}\bar{C}$

microprogrammed system [1]. A mirror image of signals from figure 4 is considered for reverse direction.

4. NUMERICAL SIMULATION

The entire commutation process is studied by numerical simulation, taking as model the SRM equations associated to PWM inverter commutation rules. The SRM equations are similar to VR stepping motor [3] and are written with the following assumptions:

- mutual inductivities are null, as shown before;
- leakage inductivities are neglected;
- self-inductivities are of sinusoidal shapes with rotor angle, as deduced from experimental measurement [1];
- magnetic saturation is neglected for an easier investigation.

The voltage equation of phase k is:

$$u_k = R_k i_k + \frac{dL_{kk}}{d\theta}\frac{d\theta}{dt} i_k + L_{kk}\frac{di_k}{dt} \qquad (2)$$

where L_{kk} is self-inductivity of phase k and θ is electrical angle, deduced from mechanical angle with:

$$\theta = z_r \theta_{mec} \qquad (3)$$

A simplified sinusoidal variation of phase inductivity is considered:

$$L_{kk} = L_0 + L_1 \cos(\theta - \frac{k-1}{2}\pi), \qquad (4)$$

where L_0 and L_1 are average, respectively amplitude of inductivity variation, which are calculated from:

$$L_0 = \frac{L_d + L_q}{2}\ ,\ L_1 = \frac{L_d - L_q}{2} \qquad (5)$$

where L_d represents the phase inductivity for aligned rotor position and L_q for unaligned position.

Mathematical model of SRM is given by state equations deduced from expression (2), where new notations appear as follows:

$$\frac{di_k}{dt} = \frac{1}{L_0 + L_1 \cos(\theta - \frac{k-1}{2}\pi)} \times$$

$$\times [u_k - Ri_k + \omega L_1 i_k \sin(\theta - \frac{k-1}{2}\pi)],$$

$$k = 1 \div 4$$

$$\frac{d\omega}{dt} = -\frac{z_r^2 L_1}{2J}\sum_{k=1}^{4} i_k^2 \sin(\theta - \frac{k-1}{2}\pi) -$$

$$-\frac{B}{J}\omega - \frac{z_r M_r}{J} sign(\omega) \qquad (6)$$

$$\frac{d\theta}{dt} = \omega$$

R - phase resistance
ω – angular speed [electrical radians/sec]
J – total rotor moment of inertia
B – coefficient of viscous friction
M_r – load torque, of reactive type.

The four voltages $u_1 \div u_4$ correspond to unipolar PWM supplying provided by a current source-type inverter. A hysteresis unit that processes the voltage between –60V and +60V with an average current up to 9A, models the PWM inverter.

The whole model of SRM drive is depicted in figure 5. This model allows 4-quadrant operation of SRM with symmetrical behavior referring to forward and reverse direction. Four modes for forward direction (normal, long-dwell, two-phase-on and brake) are implemented through manual switches. In this way it is possible on-line switching among the 4 modes and the control of forward-reverse direction. As result 4-quadrant operation of SRM can be investigated.

As control mode is periodical after 16×3.75^0 (see figure 4), a modulo 16 counter is considered in order to select the transducer signals. These signals are stored in a 16-row/4-column matrix. Mode and direction of operation are logical implemented through a Phase Logical Selection unit. Direction enabling logic generates signals for changing the operation sense.

5. SIMULATION RESULTS

Numerical specifications of SRM drive are given bellow:
$R = 0.24\ \Omega$, $L_0 = 0.007$ H, $L_1 = 0.003$ H, $M_r = 0.1$ Nm,
$J = 26 \times 10^{-6}$ Nms^2, $B = 0.001$ Nms, I=9A (phase current amplitude), $\Delta I = 0.9$ A (current PWM ripples), $V = 60$ V (supply voltage).

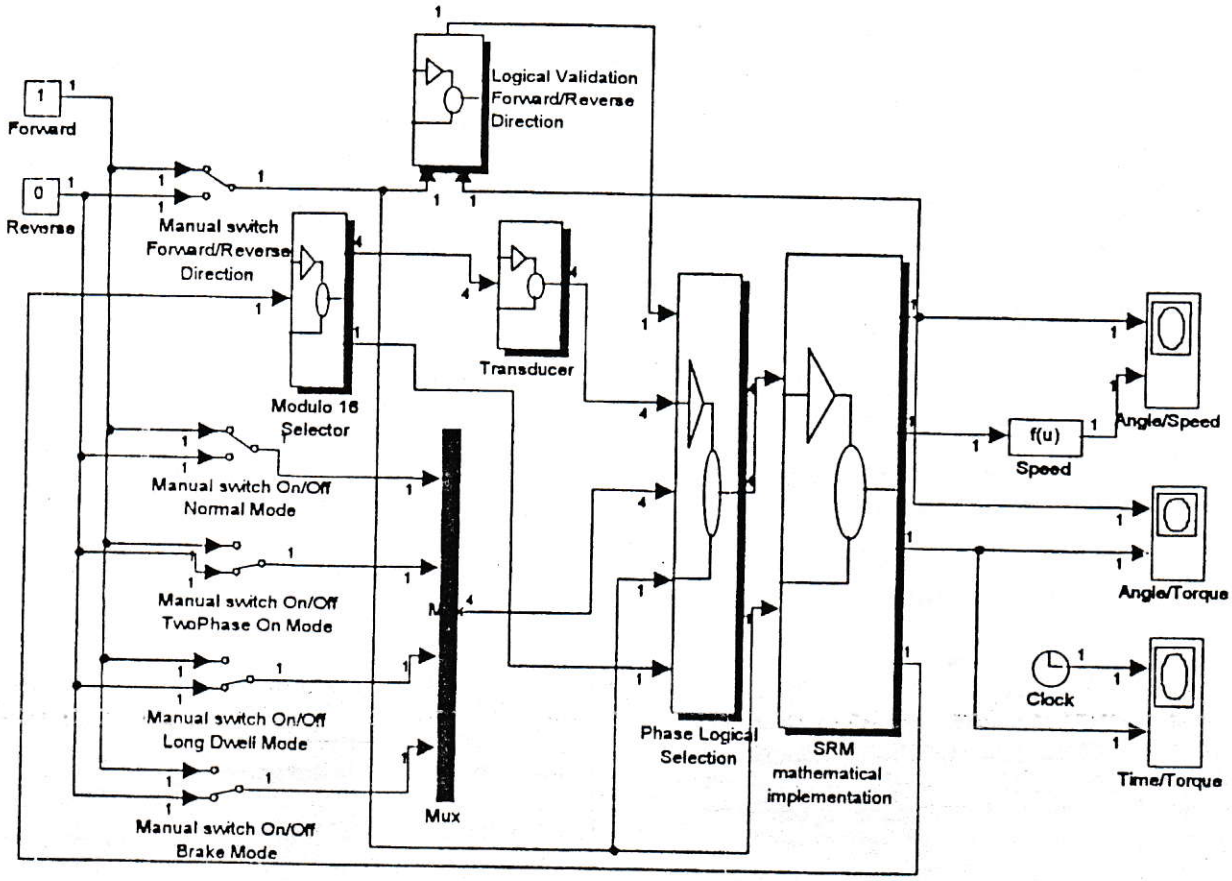

Figure 5. Simulink model of SRM

A lot of simulation results can be obtained from Simulink model. From these results, several representative curves are selected.

Figures 6 and 7 show phase voltages and currents variations during motor acceleration under constant load. Unipolar trapezoidal shapes of the currents, as result of PWM voltages are observed.

Four-quadrant operation of the SRM is shown in figures 8 and 9, with respect to speed versus angle variation and electromagnetic torque versus time variation.

Speed cycles are obtained from a sequence of modes as illustrated in figure 8: forward with normal, long-dwell and brake modes (1 and 4), backward with symmetrical modes (2 and 3). Torque variation that produces the illustrated speed cycle is given in figure 9 and comprises 12 steps such as:

I+II+III – speed cycle of quadrant 1 (figure 8)
IV+V+VI – speed cycle of quadrant 2
VII+VIII+IX – speed cycle of quadrant 3
X+XI+XII - speed cycle of quadrant 4

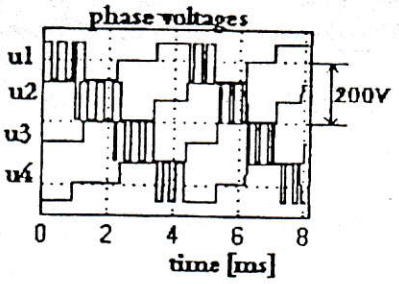

Figure 6. Phase voltages

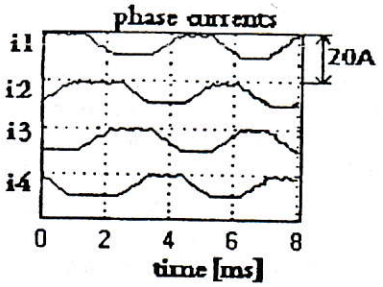

Figure 7. Phase currents

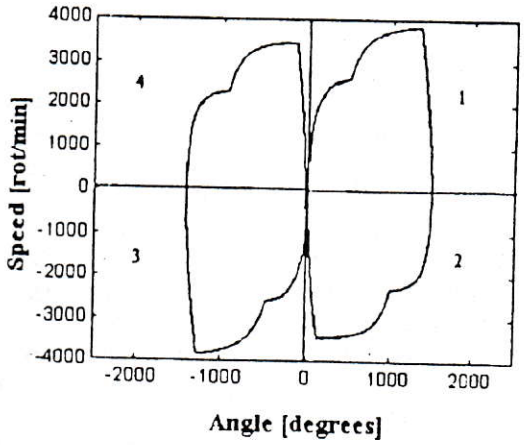

Figure 8. Speed cycles

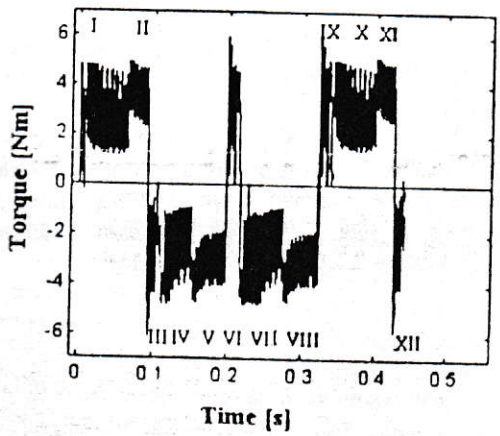

Figure 9. Torque variation

Figures 10 and 11 show the variation of speed and torque at a small time scale. As expected, at motor start the speed is influenced by the torque variation. This variation is caused by current oscillations, which are determined by both PWM ripples and trapezoidal or triangular shapes produced by sequential feeding of motor phases.

A slightly better behavior is observed in long-dwell mode, when torque ripples are smaller than in normal mode. Figure 12 shows the torque variation at motor start in long-dwell mode.

The torque ripples are now in attention of scientists, who make efforts to find methods for minimization the vibrations and noise of SRM [5].

Mechanical speed versus torque characteristics can be also deduced from Simulink model. First, SRM starting under various load torque between 0.1 and 0.4 Nm, for normal operation, is shown in figure 13. The simulation goes on until the speed is stabilized at a constant value dependant of load torque magnitude. The motor start has been also considered for long-dwell mode. As result speed/torque static characteristics are obtained, as illustrated in figure 14.

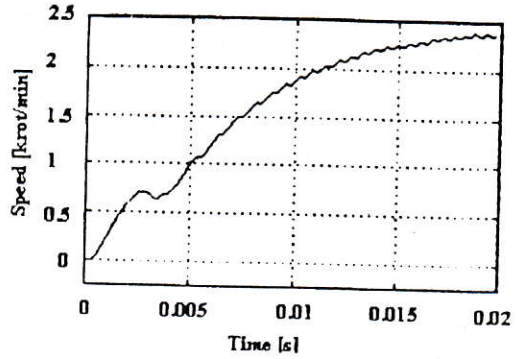

Figure 10. Speed variation in normal mode

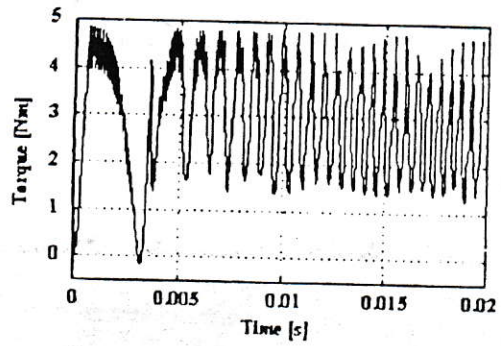

Figure 11. Torque variation in normal mode

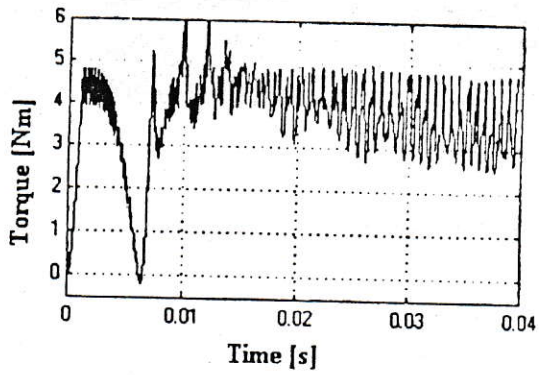

Figure 12. Torque variation in long-dwell mode

Experimental set-up arrangement consisting of 4-phase 8/6 SRM driven by a PWM inverter of current source has been considered. The control part has been built with PC-based acquisition card LabVIEW L1200, made by National Instruments [6]. Real characteristics have been obtained and a satisfactory superposition on simulated characteristics was obtained. Some differences appear for high load torque, when the influence of magnetic saturation is significant.

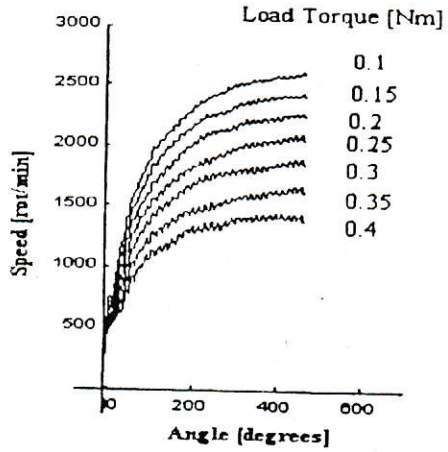

Figure 13. SRM starting in normal mode

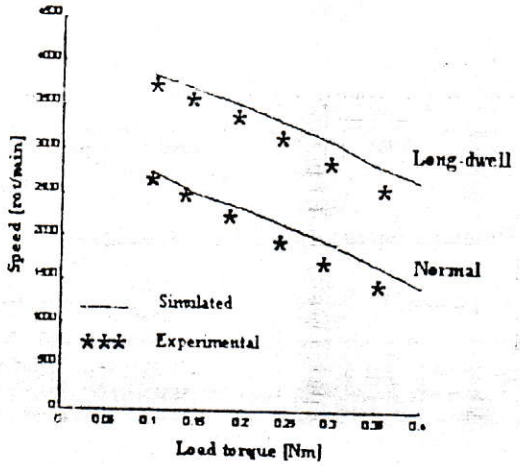

Figure 14. Speed-torque mechanical characteristics

6. CONCLUSIONS

The commutation aspects of 4-phase 8/6 SRM has been theoretically analyzed and verified by numerical simulation. Simulink model of SRM has been found most appropriate to study the commutation aspects, as they involve logic signals and combinatorial processing. A simplified mathematical model has been used with satisfactory results. A large palette of simulation procedures is available through simple manual switches. 4-quadrant operation of SRM has been investigated taking into account the variation of mechanical magnitudes such as speed and electromagnetic torque. Finally, mechanical speed versus torque static characteristics are deduced and compared to experimental ones. As observed, a good superposition is obtained.

7. REFERENCES

[1] Miller, T.J.E., "Switched Reluctance Motors and Their Control", Magna Physics Publishing and Clarendon Press, Oxford, 1993, 205 pag.

[2] Becerra, R.C., Ehsani, M., Miller, T.J.E., "Commutation of SR Motors", *IEEE Transactions of Power Electronics*, Volume 8, No.3, July 1993, pp. 257-263.

[3] Kuo, B.C., Kelemen, A., Crivii, M., Trifa, V. "Incremental Motion Control and Regulation Systems" (in Romanian), Ed. Tehnica, Bucharest, 1981, 532 pag.

[4] Trifa, V., Marschalko, R., Ramona Gălăţuş, Szekely, A., "Investigations concerning the modelling of switched reluctance motor drives", *Proceedings of A&Q International Conference on Automation and Quality Control*, Technical University of Cluj, Romania, June 1998, pp. A402-407.

[5] O'Donovan, J.G., Roche, P.J., Kavanagh, R.C., Egan, M.G., Murphy, J.M.D. "Neural Network Based Torque Ripple Minimisation in a Switched Reluctance Motor". *IEEE Transaction on Industrial Applications*, 1994, pp. 1226-1231.

[6]Trifa, V., Marschalko, R., Szekely, A., Szasz, Cs., Ramona Gălăţuş, "Investigation of a four phase switched reluctance motor supplied from a PWM inverter". *Proceedings of 6th OPTIM'98 Conference*, Brasov, Romania, Volume 2, May 1998, pp. 341-344.